Araştırma Makalesi / *Research Article* **Iğdır Üniversitesi Fen Bilimleri Enstitüsü Dergisi, 10(1): 328-337, 2020**
Kimya / Chemistry ***Journal of the Institute of Science and Technology,* 10(1): 328-337, 2020**

DOI: 10.21597/jist.548319 **ISSN: 2146-0574, eISSN: 2536-4618**

Membrane Filtration of Methyl Orange

Levent Semiz [1*]

ABSTRACT: In this work, the filtration of methyl orange by polyacrylonitrile-co-poly(2-ethylhexylacrylate) copolymer and polyacrylonitrile-co-poly(2-ethylhexylacrylate)/polyaniline membranes were utilized. It was observed that the filtration performance was improved as acrylonitrile amount in the copolymer increased. Also, functionalizing membrane with polyaniline further enhanced the dye rejection rates. Moreover, this enhancement was proportional to polyaniline amount. Furthermore, the performance of polyaniline containing membranes was pH dependent. They showed higher filtration performances at acidic mediums and they further increased as pH decreased. PAN(92)-co-P2EHA(8)- PANI(10%) membrane provided 99.3% dye rejection value for 25 ppm dye concentration at pH 2. Also, this membrane demonstrated good resistance to permeate concentration. It had 97.6% and 90.1% dye rejection rates for 50 and 100 ppm, respectively.

Keywords: Dye, filtration, membrane, methyl orange

[1] Levent SEMİZ (**Orcid ID:** 0000-0002-3218-4663), Amasya University, Vocational School of Technical Sciences, Department of Chemistry and Chemical Process Technology, Amasya, Turkey

*Sorumlu Yazar/Corresponding Author: Levent SEMİZ, e-mail: levent.semiz@amasya.edu.tr

Geliş tarihi / *Received:* 02-04-2019
Kabul tarihi / *Accepted:* 11-09-2019

INTRODUCTION

Clean water is an important issue for the environment and human health. Water pollution is a growing problem due to the decrease in clean water resources and increase in industrial progresses leading to higher wastewater. Among pollutants, dyes are one of the most water polluting waste. Dye utilizing industries such as textile, paint, leather, pharmaceutical, cosmetics and plastics cause more than $7x10^5$ ton wastewater annually (Li et al., 2015; Chen et al., 2015; Han et al., 2016; Karthik et al., 2014; Ahmad et al., 2015; Xing et al., 2015). These wastewaters are a severe threat for the environment, especially aquatic enviroment, and so for human health (Thong et al., 2018; Manimaran et al., 2018; Kumar et al., 2015). Dyes in water decreases the transmittance of light into the water and dissolved oxygen amount in aquatic environment which are essential for aquatic life (Luo et al., 2010). Moreover, azo dyes like methyl orange are carcinogenic (Kumar et al., 2018). Hence, the removal of dyes for the wastewater treatment is an important issue that should be held seriously for the environment and human health (Xu et al., 2018).

There are various methods for the removal of dyes from wastewater. Primary ones consist of oxidation, extraction, adsorption, biological treatment, ozonization, floatation, degredation, electrophoresis, coagulation, flocculation, ion-exchange, and membrane filtration (Kertesz et al., 2014; Wang et al., 2015; Ou et al., 2015; Panthi et al., 2015; Chen et al., 2018; Gao et al., 2013; Nabil et al., 2014; Liu et al., 2017; Jiang et al., 2015; Zhang et al., 2017). However, these removal methods include drawbacks such as high operation costs, low efficiency, high energy necessity, poor selectivity, technical application problems, On the other hand, membrane filtration lead to low energy requirement, low cost, lower seondary pollution, high removal efficiency, good selectivity, environmentally friendly application advantages (Chen et al., 2018; Foorginezhad and Zerafat, 2017; Aouni et al., 2012; Ong et al., 2014; Xu et al., 2016; Liu et al., 2017; Lin et al., 2015; Yao et al., 2016; Nayak et al., 2018 ; Zhang et al., 2019). In literature, different membranes have been utilized in methyl orange filtration from wastewater such as graphene oxide (GO)-nylon 6 (Chen et al., 2018), polyacrylonitrile (PAN)-tannic aci-cupric acetate (Chakrabarty et al., 2017), PAN-diamino piperazine-trimesoyl chloride (Perez-Manriquez et al., 2015), polyvinylidene difluoride (PVDF) (Mertens et al., 2018), polysulfone-polydopamine (PDA)-chitosan-SiO_2 (Ding et al., 2017), polyamide 6-GO (Chen et al., 2018), poly(arylene ether sulfone)-polyacrylic acid (Zhu et al., 2016), PAN- magnesium silicate-GO (Liang et al., 2016), PDA-polyethyleneimine-FeOOH (Lv et al., 2017), polyurethane-humic acid-chitosan (Yang et al., 2017), PAN-GO (Fathizadeh et al., 2017) and chitosan-carbon nanotube (Shi et al., 2016).

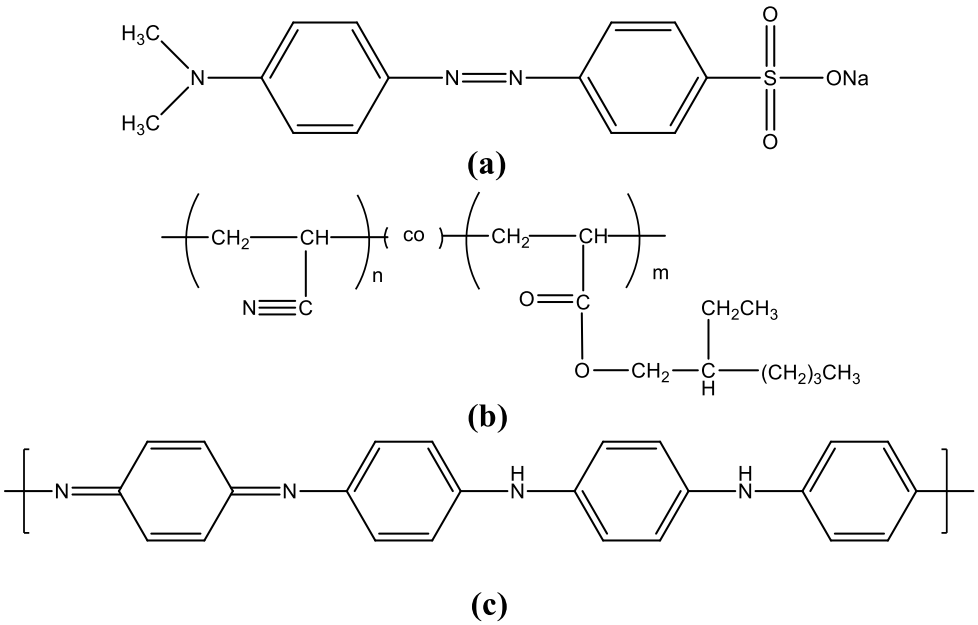

Figure 1. Chemical structures of (a) methyl orange, (b) polyacrylonitrile-co-poly(2-ethylhexylacrylate) and (c) polyaniline

In this study, methyl orange, an azo dye, filtration were utilized by polyacrylonitrile-co-poly(2-ethylhexylacrylate) copolymer and polyacrylonitrile-co-poly(2-ethylhexylacrylate)-polyaniline blend membranes (Figure 1). Effects of copolymer composition and polyaniline addition on the filtration performance were evaluated. Furthermore, pH and dye concentration effects on the dye rejection values also analyzed in this study.

MATERIALS AND METHODS

Materials

Isopropyl alcohol (99,9%), ammonium persulfate (98%), sulfuric acid (95-97%), 1-dodecanethiol (98+%), magnesium sulfate (99+%), 1-methyl-2-pyrrolidonone (99+%) and N,N-dimethyl formamide (99+%) and polyaniline (PANI) were obtained from Sigma-Aldrich and used directly without purification. 2-ethylhexylacrylate (Sigma-Aldrich, 98%) and acrylonitrile (Sigma-Aldrich, 99%) were distilled before utilization. DOWFAX 8390 and methyl orange were also used as received.

Copolymer Synthesis and Membrane Preparation

Acrylonitrile and 2-ethylhexylacrylate were copolymerized by emulsion polymerization route in order to synthesize polyacrylonitrile-co-poly(2-ethylhexylacrylate) (Bozkir et al., 2012):

20% of monomers, 1-dodecanethiol, DOWFAX 8390, 60% of ammonium persulfate and water were put into a three-naked flask having termocouple, condenser, dropping funnel, stirrer and nitrogen inlet. Temperature was raised to 66^0C and the solution was purged with nitrogen for 1 h before the compounds were mixed. The monomer mixture left was poured into the flash in 2 h. Then, the remaining ammonium persulfate was added to the flask and the solution was stirred at 66^0C. After 1 h, the copolymer was precipitated via 10 wt % aqueous $MgSO_4$ solution and washed with distilled water several times. The obtained copolymer was vacuum dried at 60^0C overnight. Copolymers were denoted as PAN(x)-co-P2EHA(y) where x and y indicate molar percents of acrylonitrile and 2-ethylhexylacrylate in the copolymer, respectively.

For the membrane preparation from copolymers, 1.2 g copolymer was dissolved in 7.7 g dimethyl formamide overnight and casted on a smooth surfaced glass. After the solution was levelled, it was put into isopropyl alcohol. After 1 h, it was immersed in distilled water and kept for overnight. In order to obtain PANI containing membranes, PANI and PAN(92)-co-P2EHA(8) copolymer were dissolved in dimethyl formamide. Then, membranes were produced via similar route described as above. For 10 wt% PANI including membrane, 0.12 g PANI and 1.08 g PAN(92)-co-P2EHA(8) were used and it was denoted as PAN(92)-co-P2EHA(8)/PANI(10%).

Membrane Characterization, Water Flux and Dye Rejection Tests

The infrared spectra of membranes were utilized by Perkin Elmer Spectrum100 FTIR spectrometer. Water uptakes were evaluated by the equation:

$$WU = \frac{m_w - m_d}{w_d} \quad (1)$$

where WU, m_d and m_w are weight percent water uptake, dry and wet weights of membranes, respectively.

Filtration tests were conducted by a dead end filtration method under the pressure of 1 bar. Permeate pH and concentrations were varied between 2-10 and 25-100 ppm, respectively. Filtration performances were utilized by Perkin Elmer Lambda 35 UV-Vis spectrometer at 465 nm (Zhu et al., 2016). Active area and thickness of membranes were about 8.0 cm^2 and 200 μm, respectively.

Flux (J) values were calculated by the following equation:

$$J = \frac{V}{At} \quad (2)$$

where V, A and are the volume (L) of the filtrate, the active membrane area (m^2) and the time interval (h), respectively.

The percent rejection of methyl orange (R) was calculated by the following equation:

$$R = \left(1 - \frac{C_f}{C_i}\right) x100 \quad (3)$$

where C_i and C_f are initial and final concentrations of methyl orange solutions before and after filtration, respectively.

The membrane morphologies were evaluated by Quanta 400F Field Emission SEM scanning electron microscope.

RESULTS AND DISCUSSION

Infrared spectra of copolymer membranes and PANI containing membranes can be seen in Figure 2. Signals at 2254 and 2925 cm^{-1} were contributed to C≡N and aliphatic C-H stretchings of PAN-co-P2EHA copolymers, respectively. Moreover, the signal at 1455 cm^{-1} was associated with C-H bending. Furthermore, peaks at 1724 cm^{-1} and 1064-1273 cm^{-1} were related to C=O and C-C-O, O-C-C stretchings, respectively. Also, signals at 1644 and 1598 cm^{-1} were pertinent to quinoid and benzoid rings of PANI. Additionally, the signal observed at 1324 cm^{-1} was related to C≡N angular deformation.

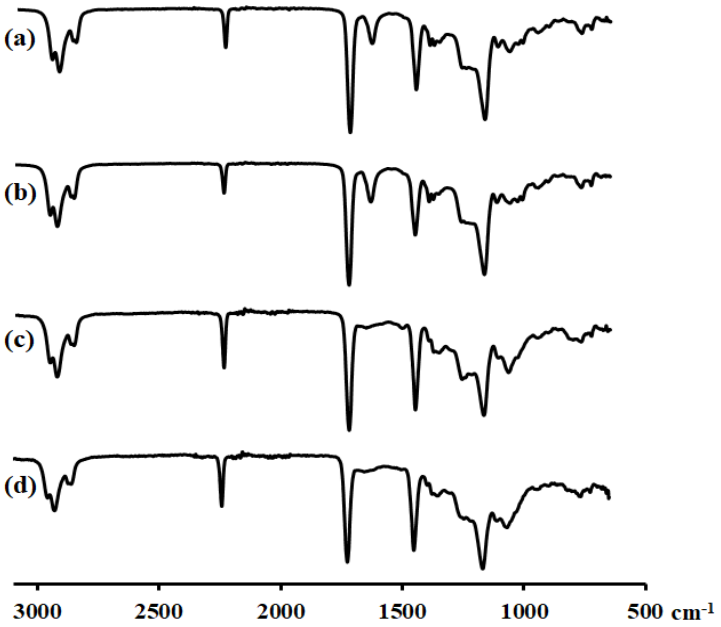

Figure 2. FTIR spectra of (a) PAN(84)-co-P2EHA(16), (b) PAN(92)-co-P2EHA(8), (c) PAN(92)-co-P2EHA(8)-PANI(5%) and (d) PAN(92)-co-P2EHA(8)-PANI(10%) membranes

PAN(92)-co-P2EHA(8), PAN(92)-co-P2EHA(8)-PANI(5%) and PAN(92)-co-P2EHA(8)-PANI(10%) membrane morphologies in Figure 3 showed that they had similar morphologies without any phase separation. Also, membranes seemed to have porous structure and pore features were estimated smaller than 100 nm. These small features provided relatively low fluxes and enhanced the filtration performance of membranes. Also, since the functionality of membranes is another important effect for effective filtration besides the small pore size, functionalization of membranes by PANI incorporation was expected to further improve the filtration performance.

In Table 1, it can be seen that water uptake values of PAN(84)-co-P2EHA(16) and PAN(92)-co-P2EHA(8) were alike. Since PANI provides hydrophilicity, PANI addition into membranes gave higher water uptake values. Also, water uptakes increased with the PANI content in the membrane. Thus, PAN(92)-co-P2EHA(8)- PANI(10%) provided the highest water uptake value of 8.89% which was 3.3 times of the water uptake of PAN(92)-co-P2EHA(8). Moreover, increase in hydrophilicity led to higher water permeation. Thus, both water and permeate fluxes increased with PANI content in the membrane. As a result, while water fluxes of PAN(84)-co-P2EHA(16) and PAN(92)-co-P2EHA(8) were calculated as 62.8 and 56.6 L m^{-2} h^{-1}, they were measured as 90.4 and 113.5L m^{-2} h^{-1} for PAN(92)-co-P2EHA(8)-PANI(5%) and PAN(92)-co-P2EHA(8)-PANI(10%), respectively. It can be seen that water fluxes were enhanced by PANI content in the membrane proportionally. Furthermore, alike results were obtained for permeate fluxes and were calculated as 44.5 and 37.8 L m^{-2} h^{-1} for PAN(84)-co-P2EHA(16) and PAN(92)-co-P2EHA(8), 68.1 and 77.3 L m^{-2} h^{-1} for PAN(92)-co-P2EHA(8)-PANI(5%) and PAN(92)-co-P2EHA(8)-PANI(10%), respectively.

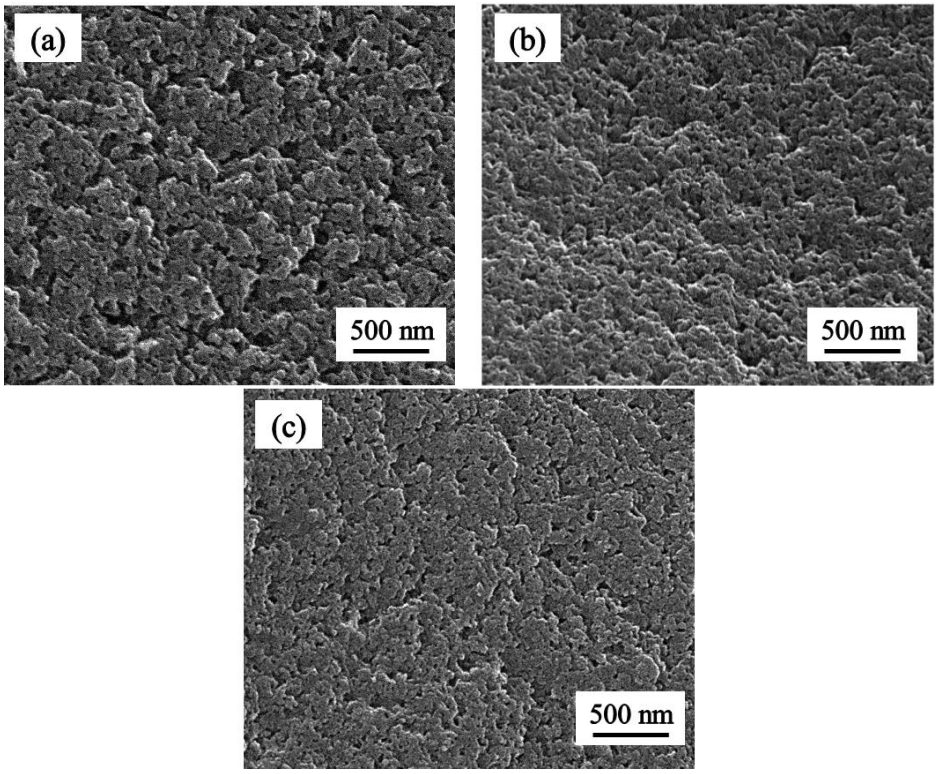

Figure 3. SEM morphologies of (a) PAN(92)-co-P2EHA(8), (b) PAN(92)-co-P2EHA(8)-PANI(5%) and (c) PAN(92)-co-P2EHA(8)- PANI(10%) membranes

Table 1. Membrane features (The permeate concentration and pH were 25 ppm and 7, respectively.)

Membrane	**Water uptake** (weight %)	**Water flux** (L m^{-2} h^{-1})	**Permeate flux** (L m^{-2} h^{-1})
PAN(84)-co-P2EHA(16)	2.61	62.8	44.5
PAN(92)-co-P2EHA(8)	2.70	56.6	37.8
PAN(92)-co-P2EHA(8)-PANI(5%)	5.88	90.4	68.1
PAN(92)-co-P2EHA(8)- PANI(10%)	8.89	113.5	77.3

The filtration performances of copolymer and PANI including membranes can be seen in Fig. 4. It shows that the filtration performance increased as the acrylonitrile content increased. This may be the result of the decrease in 2-ethylhexylacrylate amount that may lead to branching. Thus, this resulted in smaller pore features due to lower branching unit amount. In Table 1, it can be observed that both water and permeate flux values showed decrement as 2-ethylhexylacrylate amount decreased. The membrane resistance through permeation increased. This increase was also applied to dye molecules. As the acrylonitrile amount increased and fluxes decreased, the filtration performance of membranes increased. Lesser dye molecules could pass through the membrane due to the increase in membrane resistance towards permeation. The dye rejection values were measured as 38.4% and 52.8% for PAN(84)-co-P2EHA(16) and PAN(92)-co-P2EHA(8), respectively.

Since pore features and fluxes are not the only parameters that affect the filtration performance of membranes, membrane pores should be functionalized in order to enhance the rejection rates (Bozkir et al., 2012). For this purpose, PANI was added to PAN(92)-co-P2EHA(8). Figure 4 showed that PANI addition enhanced the filtration performance and this enhancement was proportional with PANI amount since higher PANI amount provided higher functionalization. Consequently, dye rejection values were calculated as 77.2% and 82.0% for PAN(92)-co-P2EHA(8)-PANI(5%) and PAN(92)-co-P2EHA(8)- PANI(10%), respectively.

In order to analyze the pH dependency of membranes towards dye rejection, pH was varied from 2 to 10. The pH of permeate adjusted to 10 for the evaluation of basicity effect on the filtration performance of membranes. It was seen that both copolymer and PANI including membranes were not sensitive to basic medium. The filtration performances at pH 10 were comparable with the ones at pH

7. On the other hand, when pH was set to 5 and medium became acidic, although the filtration performance of copolymer membranes did not showed significant changes, PANI containing membranes showed enhanced filtration performance. This may be the result of the functionality of PANI in acidic mediums. It was turned from emeraldine base form to emeraldine salt form and positively charged in acidic environments. Thus, the interaction between the positively charged membrane and negatively charged dye molecules increased. As a result, the dye rejection rates of PANI containing membranes increased with decreasing pH. Also, it was seen that this increase was proportional to PANI amount in the membrane. Dye rejection values were calculated as 84.4% and 91.1% for PAN(92)-co-P2EHA(8)-PANI(5%) and PAN(92)-co-P2EHA(8)- PANI(10%), respectively when pH was set as 5. Furthermore, when pH was dropped to 2, the filtration performance of PANI containing membranes was further improved. Also, it increased with the PANI content in the membrane and this increase was sharper when compared the one at pH 5. The filtration performance became more dependent on PANI content pH further decreased. Dye rejection values at pH 2 was found as 88.3% and 99.3% for PAN(92)-co-P2EHA(8)-PANI(5%) and PAN(92)-co-P2EHA(8)-PANI(10%), respectively.

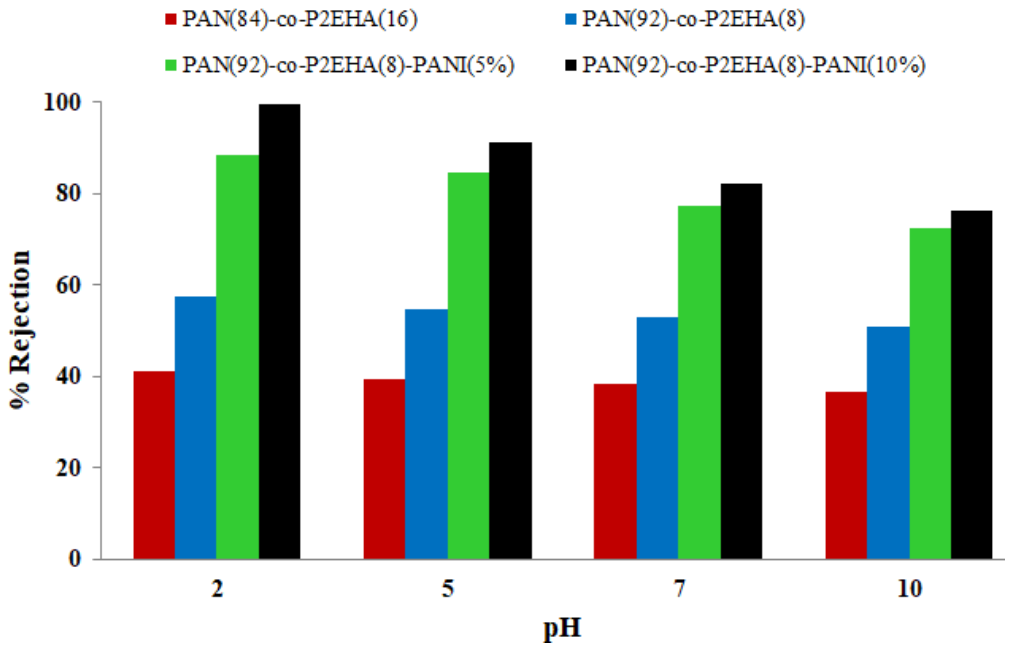

Figure 4. Dye rejection rates of PAN(84)-co-P2EHA(16), PAN(92)-co-P2EHA(8), PAN(92)-co-P2EHA(8)-PANI(5%) and PAN(92)-co-P2EHA(8)- PANI(10%) membranes at pH 2, 5, 7 and 10 (The permeate concentration was 25 ppm)

In order to analyse the concentration effect on the membrane filtration performance, PAN(92)-co-P2EHA(8)- PANI(10%) was utilized for the filtration of permeates having 25-100 ppm dye concentration at various pHs. As can be seen in Figure 5, dye rejection rates were strongly influenced by the permeate concentration at pH 7 and 10. This may be due to behaviours of copolymer and PANI in basic ant neutral mediums. The membrane was not functional and positively charged at these mediums. Thus, the interaction between dye molecules and the membrane was not strong and the filtration performance depended on pore features of the membrane. As a result, the resistance of membrane towards permeate concentration was poor. Dye rejection rates were calculated as 82.0%, 70.1%, 49.3% at pH 7 and 76.2%, 62.1%, 38.4% at pH 10 for 25, 50 and 100 ppm, respectively (Figure 5). On the other hand, when pH decreased to 5 and the environment was made acidic, the membrane showed more resistance to increase in the permeate concentration. This may arise from the conversion of PANI from emeraldine base to emeraldine salt that led to positively charged membrane. Thus, the interaction between negative dye molecules and the positive membrane enhanced. Therefore, in addition to pore features, this attraction improved the filtration performance.

Hence, dye rejection rates at pH 5 were found as 91.1%, 85.3%, and 75.3% for 25, 50 and 100 ppm, respectively. Furthermore, when pH further decreased to 2, the membrane demonstrated higher

filtration resistance towards the permeate concentration. This may be the result of the increase in the acidity of the environment and its increased effect on the functionality of PANI. The dye rejection rate was obtained as 99.3% when the permeate concentration was 25 ppm. Moreover, when the permeate concentration was increased to 50 ppm, the filtration performance of the membrane was conserved and the dye rejection value was found as 97.6%. Furthermore, even though the permeate concentration was further increased to 100 ppm, the membrane showed good resistance to this increase and its filtration performance did not show significant decrease. The dye rejection rate was measured as 90.1%. Moreover, when the rejection rates were compared with values in literature, it was observed that PAN(92)-co-P2EHA(8)-PANI(10%) could exhibit satisfactory dye rejection performance (Table 2).

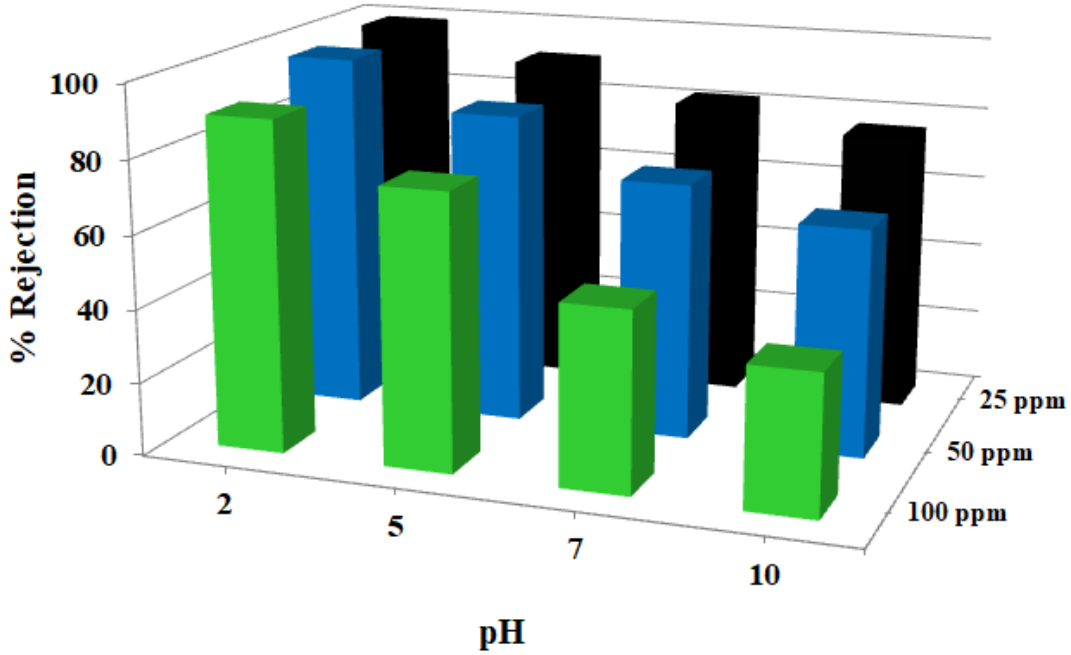

Figure 5. Dye rejection rates of PAN(92)-co-P2EHA(8)- PANI(10%) membranes against permeate concentrations of 25, 50 and 100 ppm at pH 2, 5, 7 and 10

Table 2. Methyl orange rejection rates of various membranes

Membrane	Permeate Concentration (ppm)	Dye Rejection (%)	Reference
PAN-tannic acid-cupric acetate	10	65	Chakrabarty et al., 2017
Polyamide 6 @GO@PA 6-TiO_2	10	99.36	Chen et al., 2018
PS-PDA-CS-SiO_2	20	97.6	Ding et al., 2017
Nanoclay-zeolite	20-70	10	Foorginezhad and Zerafat, 2017
Zirconia-ceramic	3000	61	Kumar et al., 2015
MgSi@RGO/PAN	100	73.4	Liang et al., 2016
PDA-polyethyleneimine-β-FeOOH	20	69.9	Lv et al., 2017
PVDF	11	80	Mertens et al., 2018
PAN-polyamide	11	30	Perez-Manriquez et al., 2015
Carboxylated MWCNTs-Chitosan	5	83.6	Shi et al., 2016
Polyurethane foam-humic acid-chitosan	5	99.7	Yang et al., 2017
GO- isophorone diisocyanate	10	97.7	Zhang et al., 2017
	25	99.3	
PAN(92)-co-P2EHA(8)-PANI(10%)	50	97.6	This study
	100	90.1	

CONCLUSION

In this study, the filtration of methyl orange by PAN-co-P2EHA and PAN-co-P2EHA/PANI membranes were utilized. It was observed that the filtration performance increased as 2-ethylhexylacrylate amount in the copolymer decreased. Furthermore, PANI addition enhanced dye rejection rates and they were proportional with PANI amount in the membrane. Also, the filtrate,on performance of PANI containing membranes further increased in acidic mediums. When pH decreased, their filtration performances improved significantly. PAN(92)-co-P2EHA(8)- PANI(10%) membrane showed the highest dye rejection rate of 99.3% at pH 2 and 25 ppm. Moreover, this

membrane demonstrated good resistance to the permeate concentration. The dye rejection rates were found as 97.6% and 90.1% when the permeate concentration increased to 50 and 100 ppm, respectively. Consequently, PAN(92)-co-P2EHA(8)- PANI(10%) may be regarded as a good alternative for the filtration of methylene orange.

ACKNOWLEDGEMENTS

This study was supported financially by The Research Centre of Amasya University under the project number FMB-BAP 17-0266.

REFERENCES

Ahmad A, Mohd-Setapar S H, Chuong C S, Khatoon A, Wani W A, Kumar R, Rafatullah M, 2015. Recent advances in new generation dye removal technologies: novel search for approaches to reprocess wastewater. RSC Advances, 5:30801-30818.

Aouni A, Fersi C, Cuartas-Uribe B, Bes-Pia A, Alcaina-Miranda M I, Dhahbi M, 2012. Reactive dyes rejection and textile effluent treatment study using ultrafiltration and nanofiltration processes. Desalination, 297:87-96.

Bozkir S, Sankir M, Semiz L, Sankir N D, Usanmaz A, 2012. High performance chromium (VI) removal from Water by polyacrylonitrile-co-poly (2-ethyl hexylacrylate) and polyaniline nanoporous membranes. Polymer Engineering & Science, 52:1613-1620.

Chakrabarty T, Perez-Manriquez L, Neelakanda P, Peinemann K-V, 2017. Bioinspired tannic acid-copper complexes as selective coating for nanofiltration membranes. Separation and Purification Technology, 184:188-194.

Chen H, Zheng Y, Cheng B, Yu J, Jiang C, 2018. Chestnut husk-like nickel cobaltite hollow microspheres for the adsorption of Congo red. Journal of Alloys and Compounds, 735:1041-1051.

Chen L, Li N, Wen Z, Zhang L, Chen Q, Chen L, Si P, Feng J, Li Y, Lou J, Ci L, 2018. Graphene oxide based membrane intercalated by nanoparticles for high performance nanofiltration application. Chemical Engineering Journal, 347:12-18.

Chen L, Li Y, Chen L, Li N, Dong C, Chen Q, Liu B, Ai Q, Si P, Feng J, Zhang L, Suhr J, Lou J, Ci L. 2018. A large-area free-standing graphene oxide multilayer membrane with high stability for nanofiltration applications. Chemical Engineering Journal, 345:536-544.

Chen X, Zhao YY, Moutinho J, Shao J, Zydney A L, He Y, 2015. Recovery of small dye molecules from aqueous solutions using charged ultrafiltration membranes. Journal of Hazardous Materials, 284:58-64.

Ding W, Zhuo H, Bao M, Li Y, Lu J, 2017. Fabrication of organic-inorganic nanofiltration membrane using ordered stacking SiO_2 thin film as rejection layer assisted with layer-by-layer method. Chemical Engineering Journal, 330:337-344.

Fathizadeh M, Tien H N, Khivantsev K, Chen J-T, Yu M, 2017. Printing ultrathin graphene oxide nanofiltration membranes for water purification. Journal of Materials Chemistry A, 5:20860-20866.

Foorginezhad S, Zerafat M M, 2017. Microfiltration of cationic dyes using nano-clay membranes. Ceramics International, 43:15146-15159.

Gao H, Kan T, Zhao S, Qian Y, Cheng X, Wu W, Wang X, Zheng L, 2013. Removal of anionic azo dyes from aqueous solution by functional ionic liquid cross-linked polymer. Journal of Hazardous Materials, 261:83-90.

Han G, Liang C-Z, Chung T-S, Weber M, Staudt C, Maletzko C, 2016. Combination of forward osmosis (FO) process with coagulation/flocculation (CF) for potential treatment of textile wastewater. Water Research, 91:361-370.

Jiang T, Liang Y-D, He Y-J, Wang Q, 2015. Activated carbon/$NiFe_2O_4$ magnetic composite: A magnetic adsorbent for the adsorption of methyl orange. Journal of Environmental Chemical Engineering, 3:1740-1751.

Karthik V, Saravanan K, Bharathi P, Dharanya V, Meiaraj C, 2014. An overview of treatments for the removal of textile dyes. Journal of Chemical and Pharmaceutical Sciences, 7:301-307.

Kertesz S, Cakl J, Jirankova H, 2014. Submerged hollowfibermicrofiltration as a part of hybrid photocatalytic process for dye wastewater treatment. Desalination, 343:106-112.

Kumar R V, Ghoshal A K, Pugazhenthi G, 2015. Fabrication of zirconia composite membrane by in-situ hydrothermal technique and its application in separation of methyl orange. Ecotoxicology and Environmental Safety, 121:73-79.

Kumar V, Karnjkar Y, George P, Singh R K, Chowdhury P, 2018. Effective removal of Congo red using sunflower oil/tri-n-octylamine system in a bulk liquid membrane process and studying the transport kinetics. Chemical Papers, 72:2055-2069.

Li P, Song Y, Wang S, Tao Z, Yu S, Liu Y, 2015. Enhanced decolorization of methyl orange using zero-valent copper nanoparticles under assistance of hydrodynamic cavitation. Ultrasonics Sonochemistry, 22:132-138.

Liang B, Zhang P, Wang J, Qu J, Wang L, Wang X, Guan C, Pan K, 2016. Membranes with selective laminar nanochannels of modified reduced graphene oxide for water purification. Carbon, 103:94-100.

Lin J, Tang C Y, Ye W, Sun S-P, Hamdan S H, Volodin A, Van Haesendonck C, Sotto A, Luis P, Van der Bruggen B, 2015. Unraveling flux behavior of super hydrophilic loose nanofiltration membranes during textile wastewater treatment. Journal of Membrane Science, 493:690-702.

Liu C, Cheng L, Zhao Y, Zhu L, 2017. Interfacially crosslinked composite porous membranes for ultrafastremoval of anionic dyes from water through permeating adsorption. Journal of Hazardous Materials, 337:217-225.

Liu M, Chen Q, Lu K, Huang W, Lü Z, Zhou C, Yu S, Gao C, 2017. High efficient removal of dyes from aqueous solution through nanofiltration using diethanolamine-modified polyamide thin-film composite membrane. Separation and Purification Technology, 173:135-143.

Luo D-H, Zheng Q-K, Chen S, Liu Q-S, Wang X-X, Guan Y, Pu Z-Y, 2010. Decolorization and degradation of reactive dye during the dyed cotton fabric rinsing process. Water Science & Technology, 62:766-775.

Lv Y, Zhang C, He A, Yang S-J, Wu G-P, Darling S B, Xu Z-K, 2017. Photocatalytic Nanofiltration Membranes with Self-Cleaning Property for Wastewater Treatment. Advanced Functional Materials, 27(1700251):1-8.

Manimaran D, Sulthana A S, Elangovan N, 2018. Reactive black 5 induced developmental defects via potentiating apoptotic cell death in Zebrafish (Danio rerio) embryos. Pharmacy and Pharmacology International Journal, 6:449-452.

Mertens M, Van Dyck T, Van Goethem C, Gebreyohannes A Y, Vankelecom I F J, 2018. Development of a polyvinylidene difluoride membrane for nanofiltration. Journal of Membrane Science, 557:24-29.

Nabil G M, El-Mallah N M, Mahmoud M E, 2014. Enhanced decolorization of reactive black 5 dye by active carbon sorbent-immobilized-cationic surfactant (AC-CS). Journal of Industrial and Engineering Chemistry, 20:994-1002.

Nayak M C, Isloor A M, Moslehyani A, Ismail N, Ismail A F, 2018. Fabrication of novel PPSU/ZSM-5 ultrafiltration hollow fiber membranes for separation of proteins and hazardous reactive dyes. Journal of the Taiwan Institute of Chemical Engineers, 82:342-350.

Ong Y K, Li F Y, Sun S-P, Zhao B-W, Liang C-Z, Chung T-S, 2014. Nanofiltration hollow fiber membranes for textile wastewater treatment: Lab-scale and pilot-scale studies. Chemical Engineering Science, 114:51-57.

Ou W, Zhang G, Yuan X, Su P, 2015. Experimental study on coupling photocatalytic oxidation process and membrane separation for the reuse of dye wastewater. Journal of Water Process Engineering, 6:120-128.

Panthi G, Park M, Kim H-Y, Lee S-Y, Park S-J, 2015. Electrospun ZnO hybrid nanofibers for photodegradation of wastewater containing organic dyes: A review. Journal of Industrial and Engineering Chemistry, 21:26-35.

Perez-Manriquez L, Aburabi'e J, Neelakanda P, Peinemann K-V, 2015. Cross-linked PAN-based thin-film composite membranes for non-aqueous nanofiltration. Reactive and Functional Polymers, 86:243-247.

Shi J, Wu T, Teng K, Wang W, Shan M, Xu Z, Lv H, Deng H, 2016. Simultaneous electrospinning and spraying toward branch-like nanofibrous membranes functionalised with carboxylated MWCNTs for dye removal. Materials Letters, 166:26-29.

Thong Z, Gao J, Lim J X Z, Wang K-Y, Chung T-S, 2018. Fabrication of loose outer-selective nanofiltration (NF) polyethersulfone (PES) hollow fibers via single-step spinning process for dye removal. Separation and Purification Technology, 192:483-490.

Wang Z, Guo J, Ma J, Shao L, 2015. Highly regenerable alkali-resistant magnetic nanoparticles inspired by mussels for rapid selective dye removal offer high-efficiency environmental remediation. Journal of Materials Chemistry A, 3:19960-19968.

Xing L, Guo N, Zhang Y, Zhang H, Liu J, 2015. A negatively charged loose nanofiltration membrane by blending with poly (sodium 4-styrene sulfonate) grafted SiO_2 via SI-ATRP for dye purification. Separation and Purification Technology, 146:50-59.

Xu H-M, Sun X-F, Wang S-Y, Song C, Wang S-G, 2018. Development of laccase/graphene oxide membrane for enhanced synthetic dyes separation and degradation. Separation and Purification Technology, 204:255-260.

Xu Y C, Wang Z X, Cheng X Q, Xiao Y C, Shao L, 2016. Positively charged nanofiltration membranes via economically mussel-substance-simulated co-deposition for textile wastewater treatment. Chemical Engineering Journal, 303:555-564.

Yang H-C, Gong J-L, Zeng G-M, Zhang P, Zhang J, Liu H-Y, Huan S-Y, 2017. Polyurethane foam membranes filled with humic acid-chitosan crosslinked gels for selective and simultaneous removal of dyes. Journal of Colloid and Interface Science, 505:67-78.

Yao L, Zhang L, Wang R, Chou S, Dong Z, 2016. A new integrated approach for dye removal from wastewater bypolyoxometalates functionalized membranes. Journal of Hazardous Materials, 301:462-470.

Zhang N, Jiang B, Zhang L, Huang Z, Sun Y, Zong Y, Zhang H, 2019. Low-pressure electroneutral loose nanofiltration membranes with polyphenol-inspired coatings for effective dye/divalent salt separation. Chemical Engineering Journal, 359:1442-1452.

Zhang P, Gong J-L, Zeng G-M, Deng C-H, Yang H-C, Liu H-Y, Huan S-Y, 2017. Cross-linking to prepare composite graphene oxide-framework membranes with high-flux for dyes and heavy metal ions removal. Chemical Engineering Journal, 322:657-666.

Zhu J, Zheng J, Liu C, Zhang S, 2016. Ionic complexing induced fabrication of highly permeable and selective polyacrylic acid complexed poly (arylene ether sulfone) nanofiltration membranes for water purification. Journal of Membrane Science, 520:130-138.